

The effects of functionalization of carbon nanotubes on toxicological parameters in mice

E Mohammadi^{1,2}, M Zeinali³, M Mohammadi-Sardoo²,
M Iranpour⁴, B Behnam^{5,6} and A Mandegary^{2,5}

Abstract

Carbon nanotubes (CNTs) have emerged as a new class of multifunctional nanoparticles in biomedicine, but their multiple *in vivo* effects remain unclear. Also, the impact of various functionalization types and duration of exposures are still unidentified. Herein, we report a complete toxicological study to evaluate the effects of single- and multiwalled carbon nanotubes (SWCNTs and MWCNTs) with either amine or carboxylic acid (COOH) surface functional groups. The results showed that significant oxidative stress and the subsequent cell apoptosis could be resulted in both acute and, mainly, in chronic intravenous administrations. Also, male reproductive parameters were altered during these exposures. The amino-functionalized CNTs had more toxic properties compared with the COOH functionalized group, and also, in some groups, the multiwalled nanotubes were more active in eliciting cytotoxicity than the single-walled nanotubes. Interestingly, the SWCNTs-COOH had the least alterations in most of the parameters. Evidently, it is concluded that the toxicity of CNTs in specific organs can be minimized through particular surface functionalizations.

Keywords

Carbon nanotubes, functionalization, oxidative stress, male reproductive toxicity, sperm, TUNEL, apoptosis

Introduction

In the last few decades, nanotechnology has opened new insights into the medical sciences, and currently, nanomedicine is introducing many practical procedures to overcome the human disease. The development of safe, multifunctional nanomaterials has been the hub of great achievements in nanomedicine.^{1–8} Diverse micro- and nanosystems ranging from well-known liposomes, niosomes, and micelles to the newly discovered carbon nanomaterials and inorganic particles such as quantum dots, gold, iron, and silica nanoparticles have been proposed in numerous studies to deliver various biomolecules.^{9–12} The extraordinary features of carbon nanotubes (CNTs) have brought them to the attention of numerous industries, which explain the several hundred tons of CNTs produced every year. This huge market for CNTs is growing annually (with a rate of 20%) and is estimated to be valued at US\$5.64 billion by 2020.¹³ On the other hand, CNTs have shown promising

¹Student Research Committee, School of Pharmacy, Kerman University of Medical Sciences, Kerman, Iran

²Department of Pharmacology and Toxicology, School of Pharmacy, Kerman University of Medical Sciences, Kerman, Iran

³Biotechnology Research Center, Research Institute of Petroleum Industry (RIPI), Tehran, Iran

⁴Pathology and Stem Cell Research Center, Kerman University of Medical Sciences, Kerman, Iran

⁵Pharmaceutics Research Center, Institute of Neuropharmacology, Kerman University of Medical Sciences, Kerman, Iran

⁶Department of Pharmaceutical Biotechnology, Faculty of Pharmacy, Kerman University of Medical Sciences, Kerman, Iran

Corresponding authors:

B Behnam, Pharmaceutics Research Center, Institute of Neuropharmacology, Kerman University of Medical Sciences, Haft-Bagh Blvd., Kerman 7616911319, Iran.

Email: behnamb@kmu.ac.ir

A Mandegary, Pharmaceutics Research Center, Institute of Neuropharmacology, Kerman University of Medical Sciences, Haft-Bagh Blvd., Kerman 7616911319, Iran.

Email: alimandegary@kmu.ac.ir

potentials in most aspects of nanomedicine and nanotechnology such as drug and gene delivery, cardiovascular research, use as antibacterials, Alzheimer's disease, imaging probes, and nanoremediation to name a few as reviewed recently, in part, by our group.^{14–20} The widespread application of CNTs, while an indicator of their value and versatility, has raised much concern about the probable consequences of their introduction into the environment and the body. Furthermore, many of the promising biomedical applications of CNTs, such as imaging, drug delivery, and cancer therapy, need direct intravenous (iv) injections of the nanotubes into the body.^{21–23} Therefore, great effort is currently being made to understand the probable adverse effects of CNTs in biologic systems while considering procedures to lower their undesirable effects.²⁴

CNTs are structurally tiny tubes of graphene layers which can be synthesized as single-walled CNTs (SWCNTs) or multiwalled CNTs (MWCNTs).^{25,26} CNTs and graphenes have shown high potential to transfer a wide range of molecules like chemotherapeutics,^{27–29} antibiotics,^{30,31} and nucleic acids^{32,33} into the cells. Pristine (the original form of CNTs after production without any surface modifications) CNTs are completely insoluble in biological solutions; therefore, numerous successful functionalization techniques have been proposed to overcome this problem.^{34,35} Among the diverse primary functionalization routes taken to prepare CNTs for attachment to other functional routes, surface oxidation, and further amination have proved more effective and popular,^{36,37} rendering the assessment of their toxicological pattern a necessity.

In addition to the surface functional groups, as previously reported by Stern and McNeil, some other major factors like number of layers, length, concentration, solvent, exposure route, and period and also synthesis method and residual catalysts could greatly influence the toxicity profile of CNTs, as seen in many other nanoparticles.³⁸ Despite the large body of data collected on the toxicology of CNTs, controversy continues to shroud much of the findings, necessitating the conduction of further studies aimed at clarifying the ultimate effects of various types of CNT.^{39,40} Proper functionalization seems to be an important step in reducing toxicity, since pristine CNTs tend to accumulate and agglomerate in organs.⁴¹ Overall, it can be concluded from the literature that current data suggest that CNTs accumulate and clear from animal organs very slowly,^{42,43}

inducing oxidative stress^{44,45} and apoptosis in cells^{46,47} and organs^{48,49} as well as inducing inflammation and epithelial granuloma formation in the lungs.^{50,51}

Although the reproductive toxicity of several nanoparticles, including carbon nanoparticles, has been studied,^{52–55} few studies were related to the male reproductive system.^{56,57} The male reproductive system is vulnerable to many exogenous compounds and environmental pollutants.⁵⁸ Therefore, the application of any nanoparticle, especially CNTs, in clinical studies on the male reproduction system calls for a robust body of in vivo research examining its impact on spermatogenesis.

Thus, in this study, we aim to evaluate the acute and subchronic (5 weeks) toxic effects of SWCNTs and MWCNTs functionalized with two core groups (carboxyl and amine) in the most important organs of mice, with special focus on spermatogenesis and the male reproductive system. Due to the importance of oxidative stress in causing the presumed toxicity, the oxidative stress parameters will also be fully investigated.

Materials and methods

Materials

Pristine MWCNTs and SWCNTs were obtained from the Research Institute of Petroleum Industry (RIPI), Tehran, Iran. Ketamine, xylazine, formalin solution (neutral buffered, 10%), trichloroacetic acid (TCA), triton X-100, *n*-butanol, 2-thiobarbituric acid (TBA), acetic acid glacial, tris-buffered saline, and hydrogen chloride were purchased from Merck Company (Germany). Evans blue, malondialdehyde (MDA), 5,5'-dithio bis-2-nitrobenzoic acid (DTNB), ethylenediaminetetraacetic acid, hydrogen peroxide, and formamide were obtained from Sigma-Aldrich (St Louis, Missouri, USA). 2,4-Dinitrophenylhydrazine (DNPH) was obtained from Scharlau Co (Barcelona, Spain). Guanidine hydrochloride was purchased from SAMCUN pure Chemical Co. (South Korea). L-Glutathione (GSH) was obtained from Solarbio Co. (Beijing, China).

Preparation of CNTs formulations

In this study, carboxylic acid-functionalized carbon nanotubes (CNTs-COOH) were obtained from our recent study and all the analyses including Fourier-transform infrared (FTIR) and transmission electron

microscopy (TEM) were stated in that report.⁵⁹ Briefly, CNTs were suspended in a concentrated sulfuric acid–nitric acid mixture (3:1 v/v) and sonicated in a bath sonicator (SONOREX, BANDELIN DT52, Berlin, Germany, with the ultrasonic frequency of 35 kHz and a nominal power of 60 W) for 4 h. The CNTs were collected as a paste on the filter and were washed with distilled water for several times. The final products, that is, SWCNTs-COOH and MWCNTs-COOH were dried at 60°C under vacuum and stored at room temperature. Amino-functionalized CNTs (CNTs-NH₂) were obtained through direct coupling of 1,6-diamino hexane with the carboxylic group of CNTs-COOH after activation with thionyl chloride (SOCl₂). Similarly, final CNTs-NH₂ (nominated as SWCNTs-NH₂ and MWCNTs-NH₂) were collected and stored as above.

Animals

Male albino mice (6 weeks old, 22 ± 2 g) were obtained from the Kerman Neuroscience Research Center, Kerman, Iran. The animals were housed in individual cages and allowed to acclimate to the environment for 4–5 days prior to the study, with a 12-h light/12-h dark cycle and free access to standard rodent laboratory diet and water ad libitum. The temperature was maintained between 21°C and 24°C, with the relative humidity of 50 ± 5%. Animal cages were kept clean and all ethical guidelines for the use of laboratory animals were followed carefully based on the national guidelines from the Ministry of Health and Medical Education of Iran. The research proposal and animal studies were all approved by the ethical committee of the Kerman University of Medical Sciences with the approval code of IR.KMU.REC.1397.273.

Study design and animal treatments

Previous report by our group⁶⁰ dealt with a single dose of 70 or 150 µg/injection of functionalized CNTs (≈3.75 or 7.5 mg/kg) and also other reports used the same range of CNTs concentrations for various purposes (≈50 µg to more than 300 µg/injection).^{51,61–63} Herein, we tried to increase the tolerable dosages and given that doses of 4 mg/kg body weight/twice a week for five consecutive weeks (i.e. 12 doses and overall 48 mg/kg at the end of study) were toxic and caused pronounced weight loss and mortality, thus the dose was decreased to once a week in this study. Therefore, one acute treatment protocol was planned in which mice were injected with the dose of 4 mg/kg on days

1, 7, and 14 (overall 12 mg/kg) and toxicological parameters were evaluated on day 15. Also, similarly, one subchronic treatment protocol was planned and injections were continued on days 21, 28, and 35 (overall 24 mg/kg) and mice were evaluated on day 36. After 1 week of acclimatization, the animals were randomly divided into 10 groups. All the male mice were roughly in the same range of weight (≈20–24 g) and they were equally and randomly to color and other properties divided into 10 groups ($n = 8$), according to a random digit table. Groups 1 and 2: vehicle control (phosphate-buffered saline (PBS)); groups 3 and 4: SWCNTs-COOH; groups 5 and 6: MWCNTs-COOH; groups 7 and 8: SWCNTs-NH₂; and groups 9 and 10: MWCNTs-NH₂ with eight mice per group and all the groups were randomly selected for the acute and subchronic protocol. CNTs were iv injected with a dose of 4 mg/kg body weight at the rate of 0.1 mL/min into the tail vein of each BALB/c mice, once a week. Mortality, behavioral changes, changes in body weights, and any signs of cholinergic toxicity were recorded during the study and compared with the control group. All animals were weighed at the beginning and at the end of each treatment. After 24 h of the last treatment, the animals were anesthetized by injecting 20% ketamine/xylazine (intraperitoneally, 1 mL/100 g body weight). Brain, Lung, liver, heart, spleen, kidney, testis, epididymis, and seminal vesicles were surgically removed, immediately washed with an ice-cold physiologic saline solution, blotted dry, weighed, and stored at –80°C for further analyses.

The sections of kidney, liver, lung, spleen, testis, and epididymis tissues were fixed in 10% formalin and embedded in paraffin. Five-micron thick sections were stained with hematoxylin and eosin (H&E) and then examined in the pathology laboratory with a Nikon light microscope (Nikon Eclipse Ti, Tokyo, Japan) with an attached digital camera (NikonDS-Ri2, Tokyo, Japan) at 400× magnification. All the experiments were repeated at least three times as individual studies.

Tissue homogenate preparation

The main organs of each mouse (liver, lung, spleen, testis, and kidney) were homogenized by T-18 Ultra Turrax Homogenizer (IKA, Germany) in a PBS buffer (0.2 M, pH = 7.4) on ice. The homogenates were centrifuged at 3000 × *g* for 15 min at 4°C to collect the supernatant. Supernatant fractions were preserved

at -80°C until the assays of MDA, carbonyl, superoxide dismutase (SOD), and total thiol content levels.⁶⁴ The protein concentrations in the supernatant were determined using the Bradford method⁶⁵ regarding bovine serum albumin as the standard.

Assessment of oxidative stress parameters

Lipid peroxidation (TBARS) assay. MDA is a product from oxidation of polyunsaturated fatty acids and can react with TBA in hot acidic conditions to produce a pink complex with maximum absorption of 532 nm.⁶⁶ Lipid peroxidation was determined on the tissues whole homogenates from control and treated animals, by estimating MDA formed with TBA and expressed as nmol/mg protein.⁶⁷ TBA reactive substances (TBARS) were measured with an ELISA, set at 532 nm and compared with standard MDA solution.

PCs contents. The oxidative damage to protein was evaluated by the determination of carbonyl groups based on the reaction with DNPH.^{68,69} The homogenate sample and 20% TCA were centrifuged at 4°C for 15 min. Pellet was incubated with 10 mM DNPH in 2 M HCl for 1 h with regular stirring. The pellets were washed with ethanol: ethyl acetate and dissolved in 6 M guanidine hydrochloride and carbonyl contents were determined from the absorbance at 366 nm using a molar absorption coefficient of 22,000/M/cm.⁶⁶

SOD activities. SOD assays were based on the ability to inhibit oxidation of oxyamine by the xanthine-xanthine oxidase system. SOD activity was determined at room temperature according to the method of Marklund and Marklund⁷⁰ with some modifications.⁷¹ SOD activity was measured at 480 nm for 4 min on an ELISA Reader ELX800 (BioTek, Vermont, USA). The unit of activity is defined as the amount of enzyme that inhibits the rate of autooxidation of pyrogallol by 50% under standard conditions and was expressed as U/mg protein.

Total GSH content. Total GSH content in tissues was measured by the method of Hu⁷² with some modifications⁷³ by using DTNB. Sample concentrations of GSH were determined from the standard curve. The chromophoric product resulting from the reaction of the reagent with GSH, that is, 2-nitro-5-thiobenzoic acid possesses a molar absorption at 412 nm. The concentration of GSH in tissues was expressed as $\mu\text{mol/mg}$ protein.

TUNEL assay. For detection of apoptosis at the cellular level and based on labeling of DNA strand breaks, the terminal deoxynucleotidyl transferase dUTP nick end labeling (TUNEL) kit (Roche, Germany) was used. For TUNEL assay, mice were in the subchronic group, that is, they received 4 mg/kg of CNTs with the accumulative dose of 24 mg/kg. The paraffin sections were dewaxed and rehydrated by standard methods. Protease K was added and incubated for 30 min at 37°C . Positive control sections were incubated for 10 min in DNase 1. The sections were incubated with TUNEL reaction mixture. Antifluorescein-alkaline phosphatase was added and incubated for 30 min at 37°C . Subsequently, the sections were washed in PBS and incubated for 20 min with the substrate. They were analyzed by light microscopy. The apoptotic indexes of 100 randomly selected tubules were evaluated, and the mean apoptotic index of each case was calculated.⁷⁴

Assay for caspase-3 activation. To explore the potential mechanism of CNTs-induced apoptosis, the relative levels of key apoptosis-related protein (caspase 3) were evaluated by western blot analysis. For caspase-3 assay, mice were in the subchronic group, that is, they received 4 mg/kg of CNTs with the accumulative dose of 24 mg/kg. Tissues were homogenized in an ice-cold PBS and protease inhibitor. After determining protein concentration with Bradford assay, 30–50 μg protein (30 μg for liver and lung and 50 μg for testis) was loaded onto a 12–15% sodium dodecyl sulfate-polyacrylamide gel and separated by electrophoresis, and finally, proteins were transferred to polyvinylidene difluoride membranes (Roche, Germany). The membranes were blocked with 5% nonfat dry milk and then probed with the primary antibodies: anti-caspase-3 (9662s; Cell Signaling Technology, Danvers, Massachusetts, USA) and β -actin antibody (sc-47778; Santa Cruz Biotechnology, Dallas, Texas, USA) at 4°C overnight under constant rotation. The membrane was then washed three times with tris-phosphate buffer saline (TPBS; PBS and 0.1% Tween 20), incubated further with secondary antibody (anti-rabbit and anti-mouse) at room temperature and then washed three times with TPBS. The immunoblot was visualized by the use of an enhanced chemiluminescence detection kit (Roche, Germany).

Sperm extraction. The cauda epididymis part of mice was chosen for sperm count and motility. Cauda

epididymides were minced and incubated for 20 min at 37°C in an atmosphere of 5% CO₂ in 2 mL of preincubated Roswell Park Memorial Institute (RPMI) Medium and allowed to extract the activated sperms.

Sperm motility. Well-mixed fresh sperm suspension (10 µL) was put in the center of the lower glass and immediately was covered. First, the motile spermatozoas within the area of the grid were counted and then the immotile spermatozoas which did not show any movement were counted under the microscope (BIO1 Microscopes, BEL Engineering, Italy).⁷⁵ Data were expressed as the percentage of motile sperms.⁷⁶

Sperm count. The sperm suspensions were diluted 1:20 in a diluting solution (sodium bicarbonate and formalin in distilled water) to be counted by Neubauer-type hemocytometer under the microscope. Mature spermatids were counted in a Neubauer chamber (four fields per each group was analyzed).

Sperm viability and morphology. A total of 10 µL from each sample was mixed with 10 µL of 0.5% eosin Y stain on a glass microscope slide and the suspension was incubated for 30 s at room temperature (20°C) where it was smeared by sliding a coverslip. Light microscopy was used to determine the percentage of viable sperm as the live sperms remained white while dead sperms were stained red.⁷⁷ The morphology was regarded as normal when the acrosome was curved like a hook, and the neck was straight with a free-end single tail. Morphology was regarded as abnormal when the head was smaller than the normal state or without curvature, the neck was broken, and the tail was isolated or rolled into a spiral form or was cut.⁷⁸

Evaluation of BTB permeability. Blood–testis barrier (BTB) was evaluated by the Evans blue extravasation method.^{79,80} Evans blue (2% in saline, 3 mL/kg; Sigma-Aldrich) was given iv at 3 h before sacrificing followed by transcardial perfusion of NaCl 0.9% to remove the intravascular dye from the vessels until the drainage was colorless. Afterward, one testis was removed, weighed, dried in a desiccator oven for 48 h at 60°C, and reweighed. Dried tissue was incubated in *N,N*-dimethylformamide (Sigma-Aldrich) in 60°C water bath for 24 h. Evans blue content was determined in the supernatants at 632 nm using a spectrophotometer (JENWAY 6505 UV-vis spectrophotometer, Staffordshire, UK). Absorbance was compared with a standard curve of 0.05–25 mg/mL Evans blue in *N,N*-

dimethylformamide. Extravasation is expressed as nanogram of Evans blue per milligram of dry weight. Another testis was sectioned into slices (10 µm in thickness) by freezing for an examination of BTB integrity. Evans blue entrapped in the sections of testis and showed an emission light at 595 nm while being excited at 540–580 nm in a fluorescence microscope (Nikon Inverted Microscope Eclipse Ti-U, Nikon Instruments, Tokyo, Japan). Positive controls were animals that received cadmium chloride IP at a dose of 5 mg/kg body weight 24 h before Evans Blue injection.

Histopathological evaluation. Histopathology of the lung, liver, spleen, kidney, testis, and epididymis was studied with the H&E staining with subsequent light microscopy examination. Tissue samples were fixed in 10% formalin solution, and after 24 h were passed in a series of graded ethanol, and embedded in paraffin blocks. Paraffin sections were cut into 5-µm thick slices and placed onto glass slides.

Statistical methods

The presence of significant differences between mean groups was determined using analysis of variance with Scheffé's S method as the post hoc test. The experimental results were expressed as mean ± standard deviation (SD). Statistical differences between groups were determined by the Student's *t*-test. *p* Values less than 0.05 were regarded as statistically significant. All statistical tests were performed using the Statistical Package for Social Sciences (SPSS, version 18).

Results

CNTs preparations

Our previous report showed that based on the mentioned synthesis protocol, the mean diameters for most SWCNTs and MWCNTs were determined to be 10 and 16 nm, respectively.⁵⁹ The lengths of CNTs preparations were about 1–10 µm. Zeta potentials for pristine CNTs and CNTs-COOH and CNTs-NH₂ preparations were about -25, -39, and -16 mV, respectively. A reduction in zeta potentials in CNTs-COOH and an increase in zeta potentials in CNTs-NH₂ could be related to their surface charges. All formulations were analyzed for any precipitation after 1 min, 30 min, 60 min, and 30 days of synthesis and dispersion through bath sonication (Figure 1). CNTs-NH₂ groups started to sediment after 30 min while CNTs-COOH

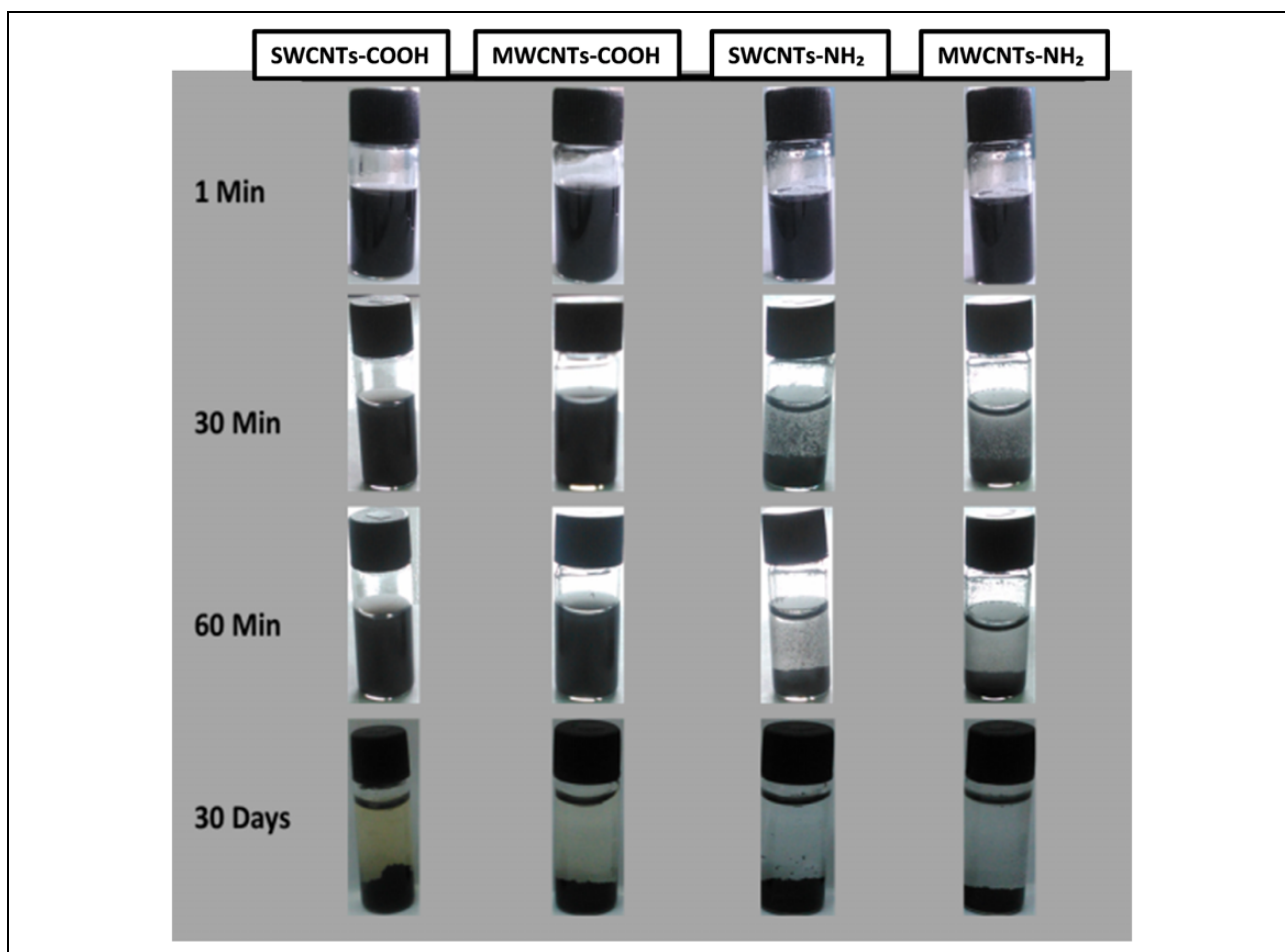


Figure 1. Nanoparticles stability in CNTs formulations over different time periods is presented. CNT: carbon nanotube.

groups showed this sedimentation near 60 min after dispersion. Also, almost all of the nanotubes sedimented during 1 month of storage.

Mortality and behavioral changes

Primary injection of CNTs-NH₂ was accompanied by agitation in mice and showing aggressive behaviors. The rate of mortality was 15% and 22% for SWCNTs-NH₂ and MWCNTs-NH₂, respectively. Some behavioral changes were also seen in the MWCNTs-COOH group without mortality. Surprisingly, the SWCNTs-COOH group (and of course the control group) did not show any abnormal behavior changes, and no mortality was seen in this group. Body weight and relative weights of liver, lung, spleen, kidney, testis, seminal vesicle, and right epididymis in control and treatment groups are presented in Figure 2. Body-weight significantly decreased ($p < 0.05$, 35-day post-treatment) in the two CNTs-NH₂ groups compared with the control. On the other hand, CNTs-COOH

groups did not show any significant change in body weight. Liver, lung, and spleen weights increased insignificantly at 15- and 35-day posttreatment. There were no differences in weights of the brain, heart, kidneys, testes, epididymes, and seminal vesicles at the end of the experiment among the treated groups.

Effect of CNTs on oxidative stress

Significant alterations in tissue levels of TBARS were found in almost all of the CNTs-exposed cases in comparison to control subjects (Figure 3(a)). Also, during the subchronic phase, the increasing effects of CNTs on TBARS were higher for CNTs-NH₂ groups compared with the CNTs-COOH groups ($p < 0.01$). Protein carbonyl (PC) levels (Figure 3(b)) were significantly ($p < 0.05$) elevated by MWCNTs-COOH, SWCNTs-COOH, and also by SWCNTs-NH₂ and MWCNTs-NH₂ ($p < 0.001$), in almost all of tissues in comparison to the control. However, during the acute phase, SWCNTs-COOH did not show

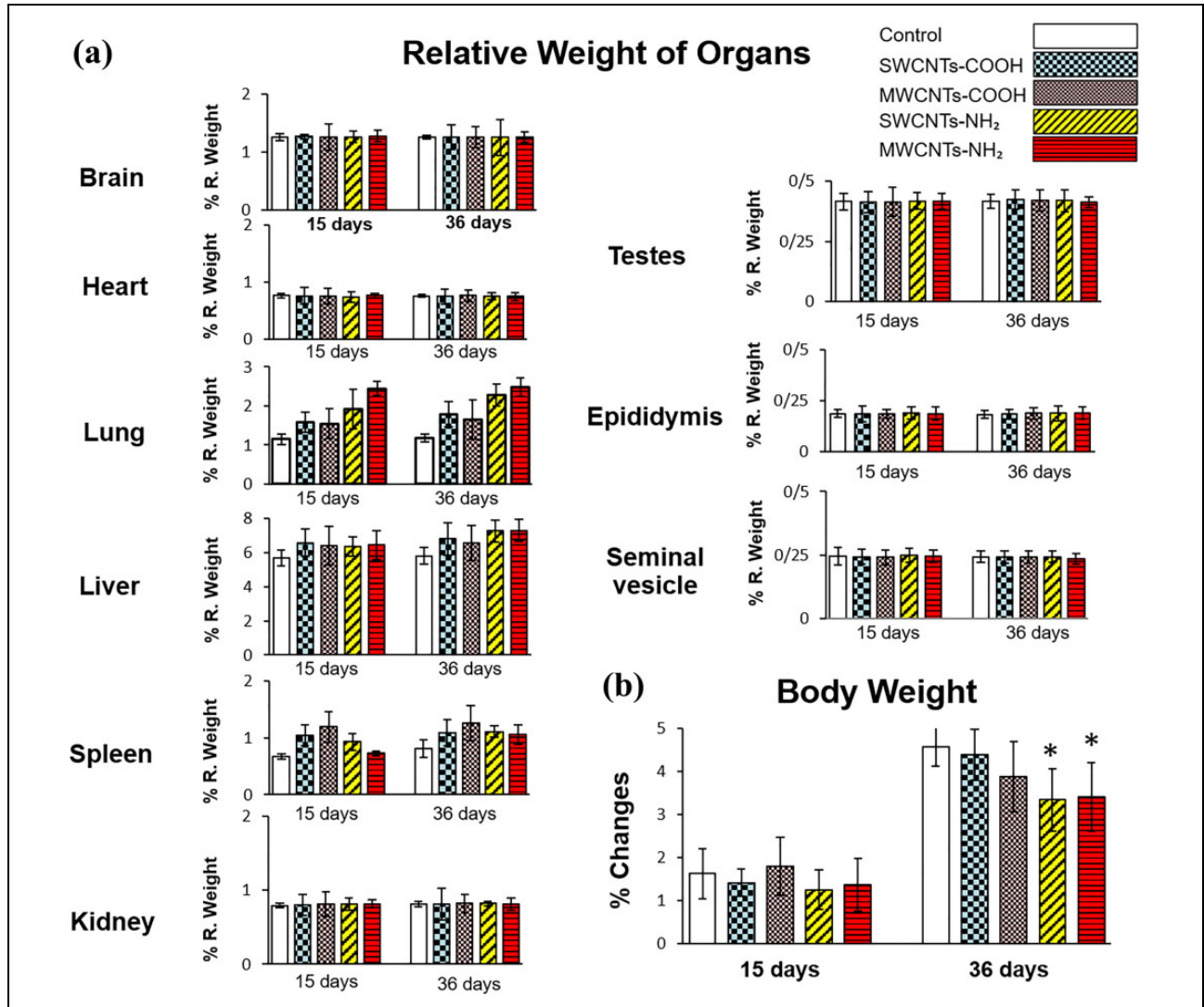


Figure 2. Body and organ weight. (a) Relative organ's weight at days 15 and 36. (b) Body weight changes (percent) at days 15 and 36. Data are reported as mean \pm SD ($n = 8$ mice per group). * $p < 0.05$ versus control. SD: standard deviation.

any significant alteration of PC levels except in the lung. The SOD activity of all organs (Figure 4(a)) was significantly reduced in CNTs-COOH ($p < 0.01$) and CNTs-NH₂ ($p < 0.001$) in relation to control. GSH levels were measured (Figure 4(b)) and results stated that similar to the above trend, GSH levels had also decreased significantly in the treatment groups compared with the control group treated with normal saline. Moreover, CNTs-NH₂ significantly decreased the GSH levels in all organs of the experimental mice more than the CNTs-COOH group did.

Histopathology

Histopathology of the lung, liver, spleen, and kidney. The results from the histopathological examination of

lungs, liver, spleen, and kidneys after treatment with two doses of CNTs, the groups were scored using the following criteria: minimal, mild, moderate, and severe. There were no severe pathological findings in any of the sections and most of the findings showed mild and moderate changes mostly in the 35-day treatment groups. Animal lungs exhibited moderate fibrosis, congestion, perivascular, and peribronchial inflammation in a dose-dependent manner in CNTs-NH₂ groups while these changes were also evident in CNTs-COOH groups but to a mild degree (Figure 5(a) to (g)). Liver results indicate a similar trend to the lung findings as the CNTs-NH₂ groups were more prone to induce moderate changes in comparison to the CNTs-COOH groups (Figure 5(h) to (n)). In both

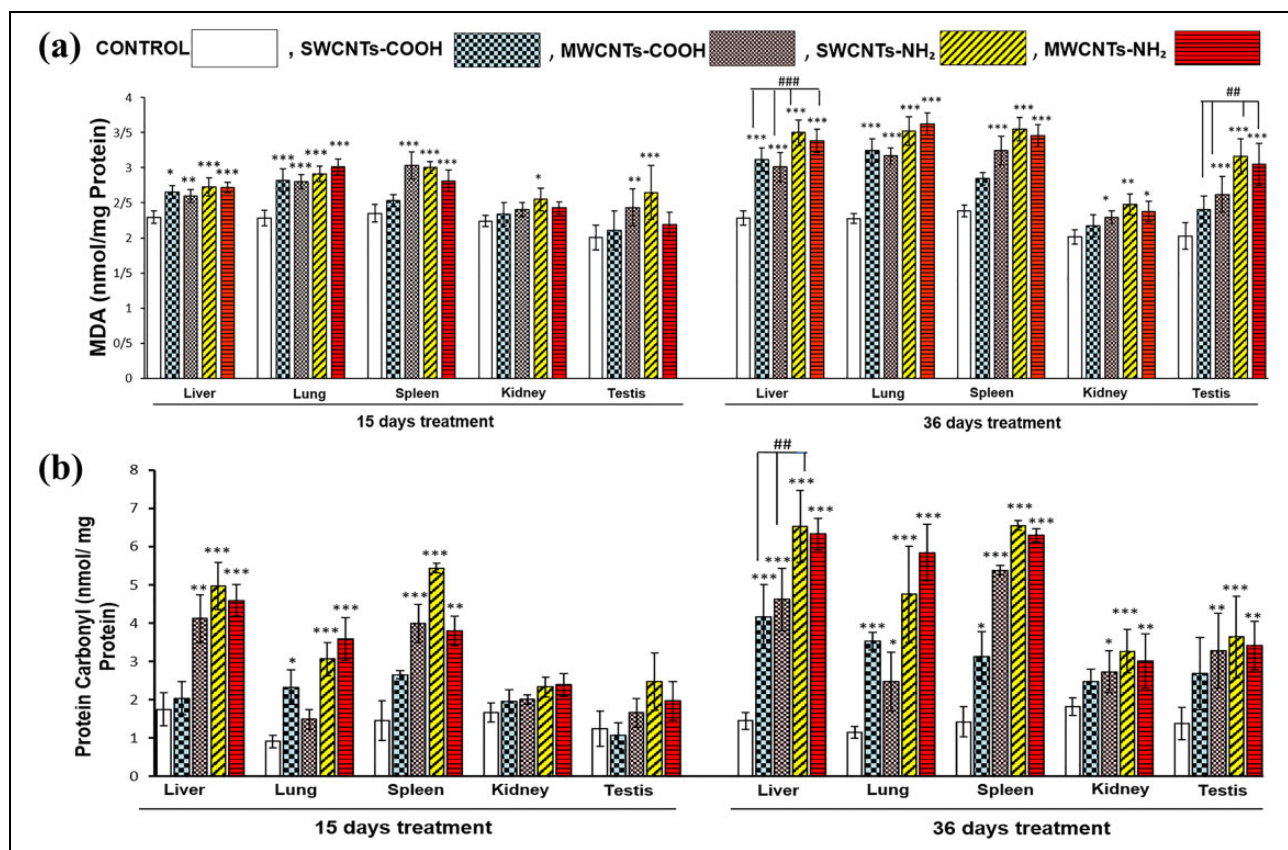


Figure 3. Effects of CNTs (4 mg/kg) for 15 days (accumulative dose: 12 mg/kg) and 36 days (accumulative dose 24 mg/kg) on the oxidative stress parameters. (a) MDA concentration and (b) PC concentration in liver, lung, kidney, spleen, and testis. Values are expressed as mean \pm SD, for $n = 8$. * $p < 0.05$; ** $p < 0.01$; *** $p < 0.001$ compared with control and # $p < 0.05$; ## $p < 0.01$; ### $p < 0.001$ compared with other CNTs groups. CNT: carbon nanotube; MDA: malondialdehyde; PC: protein carbonyl; SD: standard deviation.

organs, the lesions were clearly fewer at lower administered doses. Moreover, the accumulation of nanotubes had taken place in Kupffer cells and alveolar macrophages of liver and lung, respectively. Spleen samples showed moderate congestion and mild tortuous splenic sinusoids (TSS) in CNTs-NH₂ groups and mild congestion and TSS in the MWCNTs-COOH group. SWCNTs-COOH showed minimal changes, and no CNTs aggregates and necrosis were found in the spleens of any treated groups. The kidney samples did not show any specific morphological and pathological changes, except moderate inflammation and congestion in the CNTs-NH₂ and mild congestion without inflammation in CNTs-COOH groups, without accumulation (data not shown). Simple photographs were also taken of organs after 5 months of the final dose without carrying out pathological studies (Supporting information, Figures S1 and S2). Morphological findings indicated that tissue color could

turn from black to an almost normal state in some groups (mostly in SWCNTs-COOH) during this time, and this might be a sign of gradual elimination of nanotubes.

Histopathology of the testes and epididymes. Representative micrographs of seminiferous tubules in different groups are shown in Figure 6(a) to (f). Histological study of testes demonstrated considerable changes in CNTs-NH₂-treated animals as compared with the control in a dose-dependent manner (Figure 6(b) to (d)). Findings include seminiferous tubules with vacuolization, degeneration, edema, and reduced thickness of the germinal epithelium. Spermatogenic cells decreased in some seminiferous tubules of testes. The thickness of the germinal epithelium was drastically reduced in some of the tubules due to tubular degeneration. Moreover, many seminiferous tubules in CNTs-NH₂ groups showed

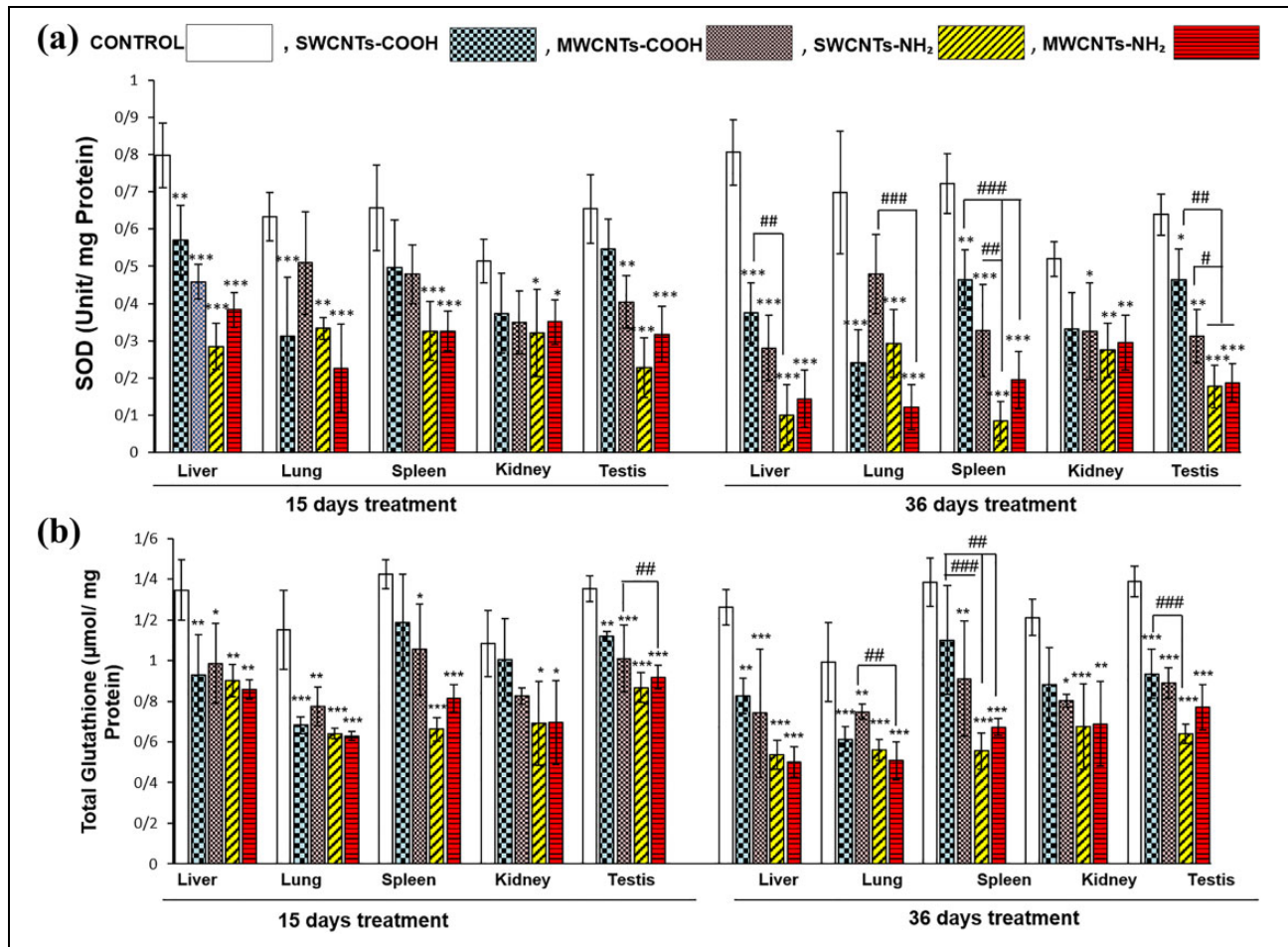


Figure 4. Effects of CNT (4 mg/kg) for 15 days (accumulative dose: 12 mg/kg) and 36 days (accumulative dose 24 mg/kg) on the oxidative stress parameters. (a) SOD and (b) GSH activity in liver, lung, kidney, spleen, and testis. Values are expressed as mean \pm SD, for $n = 8$. * $p < 0.05$; ** $p < 0.01$; *** $p < 0.001$ compared with control and # $p < 0.05$; ### $p < 0.01$; #### $p < 0.001$ compared with other CNTs groups. CNT: carbon nanotube; SOD: superoxide dismutase; SD: standard deviation; GSH: glutathione.

germ cell disorganization with necrotic cellular debris. Similar to other pathological results, MWCNTs-COOH exposure led to mild testicular hypertrophy, and no lesion was present in the SWCNTs-COOH group (Figure 6(e) and (f)). The epididymes of exposed mice were indicative of congestion and edema in CNTs-NH₂ groups while changes were much fewer in the CNTs-COOH-treated animals (Figure 6(g) to (k)). Also, a considerable reduction in sperm count was seen in amino-functionalized groups.

Sperm characteristics. Epididymal sperm count (Figure 7(a)), motility (Figure 7(b)), and viability (Figure 7(c)) are shown for control- and CNTs-treated groups. Treatment of male mice with almost all CNTs groups caused a significant decrease in

sperm concentration, motility, and viability 35-day posttreatment. We observed that CNTs treatment impaired sperm morphology (Figure 7(e) and (d)). SWCNTs-COOH treatment did not cause significant sperm abnormalities. While the MWCNTs-COOH, SWCNTs-NH₂, and MWCNTs-NH₂ groups had significantly higher abnormalities compared with the control group.

BTB integrity. BTB integrity was determined by Evans blue extravasation method by reading the absorbance at 632 nm. All CNTs groups except the SWCNTs-COOH caused a significant increase in Evans blue extravasation in testis tissue only in the 36-day treatment protocol compared with the control (Figure 8).

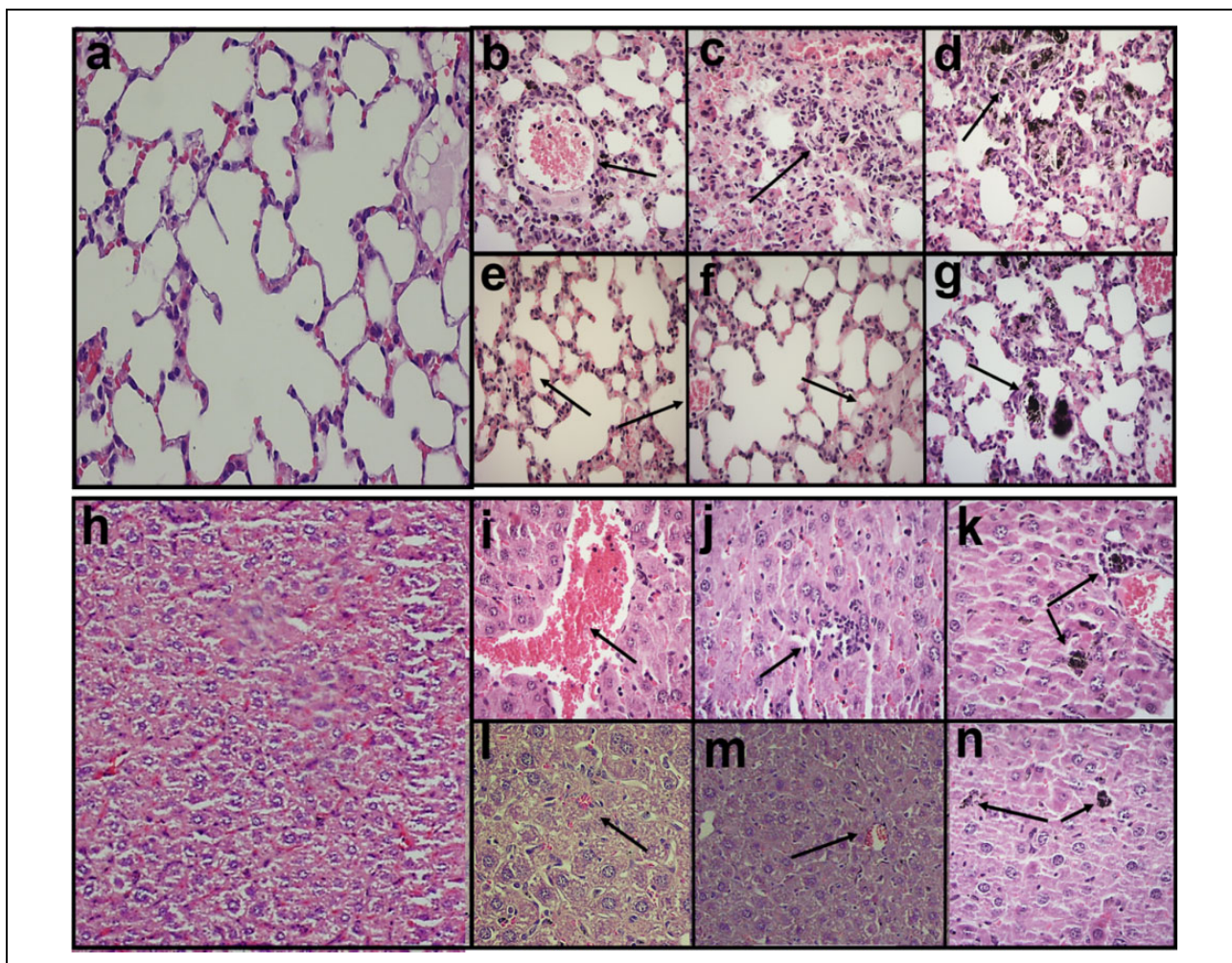


Figure 5. The lung and liver histology investigation after exposure to CNTs. Lung histology: (a) control. (b)–(d) CNTs-NH₂ groups: (b) congestion, (c) fibrosis, and (d) sedimentation of CNTs in lung. (e)–(g) CNTs-COOH groups: (e) congestion, (f) fibrosis, and (g) sedimentation of CNTs in the lung (40× scale bar). Liver histology: (h) control. (i)–(k) CNTs-NH₂ groups: (i) congestion, (j) inflammation, and (k) sedimentation of CNTs in liver. (l)–(n) CNTs-COOH groups: (l) and (m) congestion and (n) sedimentation of CNTs in the liver (40× scale bar). CNT: carbon nanotube; NH₂: either amine; COOH: carboxylic acid.

Apoptosis. The involvement of apoptosis in testes was examined as a function of time over 36 days by using the TUNEL test. TUNEL cells (brown) were visible in the positive control (Figure 9(a2)), while in the negative control, no signal was detected (Figure 9(a1)). Few TUNEL positive cells (TUNEL⁺) were detected in SWCNTs-COOH (Figure 9(a3)), and apoptotic cells were mostly germ cells and were observed in MWCNTs-COOH, SWCNTs-NH₂, and MWCNTs-NH₂ groups (Figure 9, (a4) to (a6)).

In vivo apoptosis evaluation was also determined in other organs as depicted in Figure 10. The results from Western blot analysis showed that the amount of cleaved caspase-3, indicative of caspase-3 activation,

significantly increased in most of the treated groups compared with the control group. These data show that treatment with CNTs could elicit enhanced apoptosis although it was mainly in the SWCNTs-NH₂ and MWCNTs-NH₂ groups.

Discussion

The unique physicochemical properties of CNTs make them attractive for diverse therapeutic applications.^{81–84} In spite of numerous interesting biomedical applications of CNTs, their clinical studies in humans are still limited by inadequate safety requirements and toxicological data.^{85–87} Advanced functionalized CNTs could improve the biological compatibility of

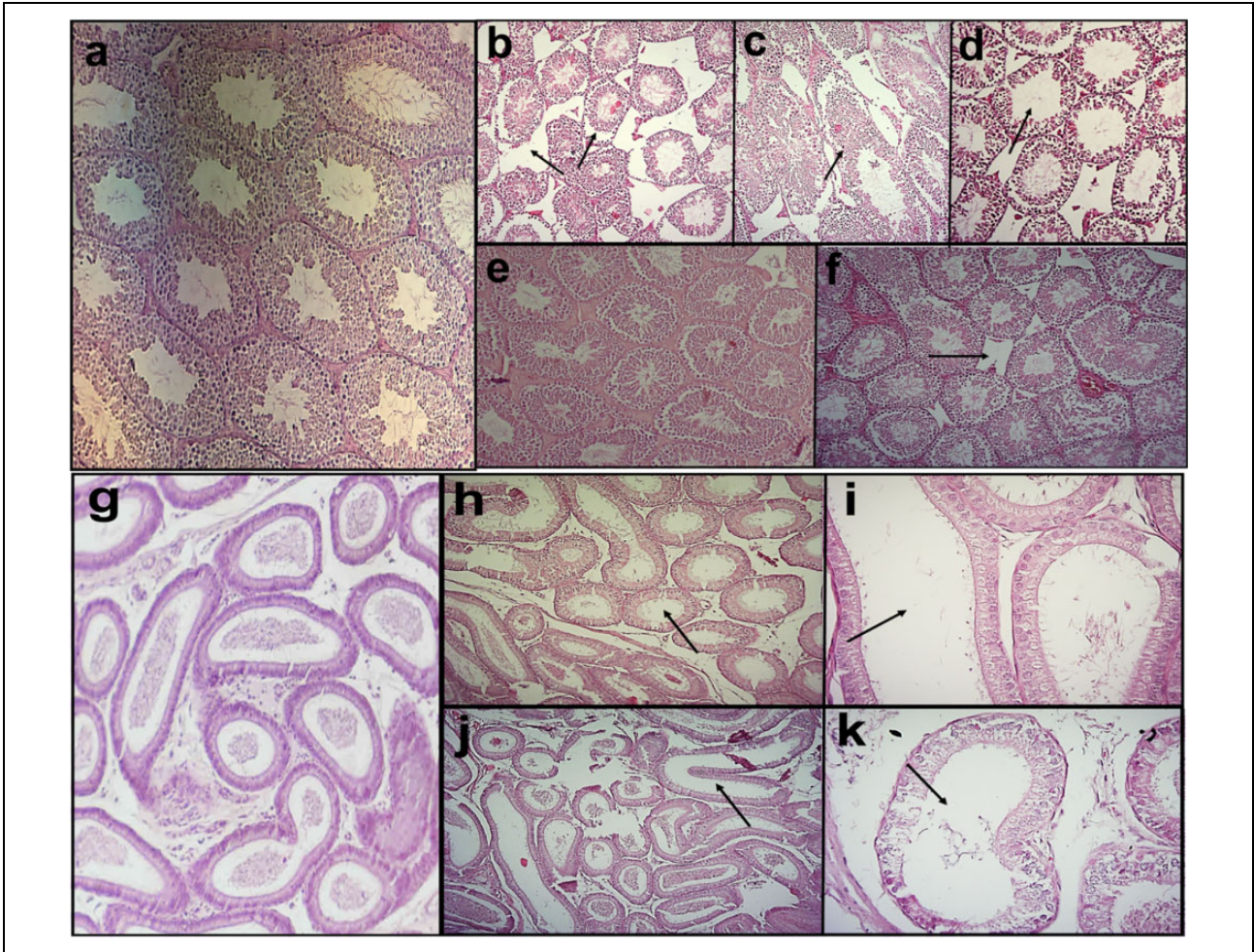


Figure 6. Histopathology of testis and epididymis of control- and CNTs-treated mice. Testis histology: (a) control. (b)–(d) CNTs-NH₂ groups: (b) testicular tubular atrophy (20× scale bar), (c) necrosis (40× scale bar), and (d) decreased germinal epithelium and spermatogenesis. (e) and (f) CNTs-COOH groups: (e) normal seminiferous tubules and (f) mild testicular tubular atrophy (20× scale bar). Epididymis histology: (g) control (40× scale bar). (h) and (i) CNTs-NH₂ groups and (j) and (k) CNTs-COOH groups (scale bar 40× and 200×). CNT: carbon nanotube; NH₂: either amine; COOH: carboxylic acid.

nanotubes and pave the way to many medical applications.^{88,89} Recently, different aspects of CNTs toxicity have become extremely important; for example, El-Gazzar et al. showed MWCNTs are more toxic than double-walled carbon nanotubes.⁹⁰ Chemical functionalization of CNTs with COOH or NH₂ groups displays effective methods to enhance water solubility and dispersibility.^{91,92} Therefore, functionalized CNTs are generally more biocompatible than pristine CNTs because of improved hydrophilicity and greater dispersion in biological media.^{89,93} Numerous *in vitro* and *in vivo* toxicity studies of functionalized CNTs have supported this concept in addition to exploring the *in vivo* fate of COOH, NH₂, and pluronic-functionalized CNTs.^{89,94}

However, the effects of surface charges of CNTs when they interact with tissue and cells are not comprehensively understood. In the present study, we first studied the effects of different surface functionalizations and also the number of nanotube walls in mice, in association with oxidative stress and apoptosis in main target organs and also investigated the effect of CNTs on the male reproductive system.

Conversely, some studies suggest that functionalization allows for better dispersion of CNTs in biological fluids, thus increasing their toxicity potential. For example, Saxena et al. reported that aspiration of well-dispersed SWCNTs-COOH caused greater inflammation than pristine CNTs in mice.⁹⁵

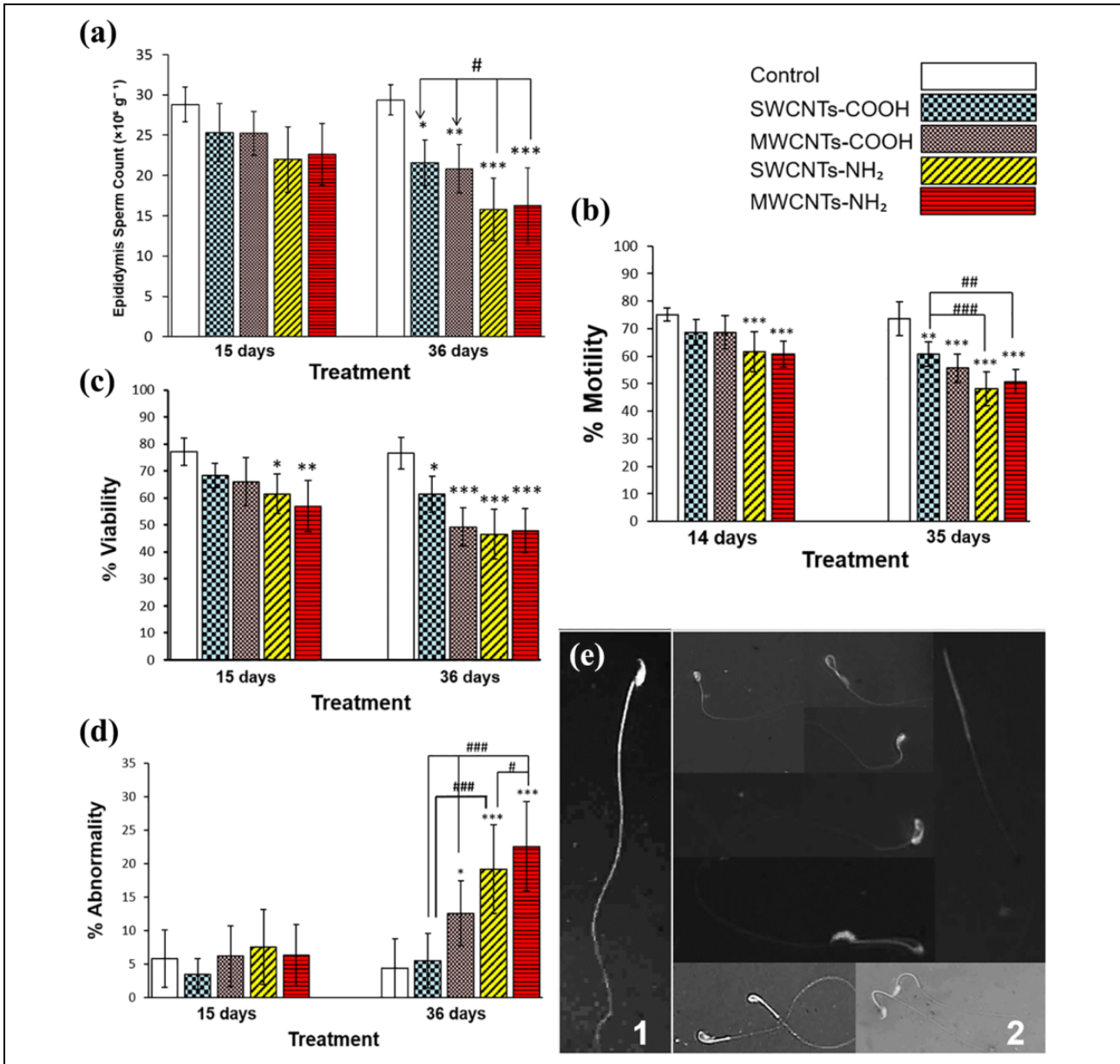


Figure 7. Effect of CNTs on sperm characterization. (a) Sperm's count, (b) motility, (c) viability, (d) the quantification of abnormal sperms, and (e) types of sperm-shape abnormalities found in CNTs-treated mice. (e1) Normal sperm with a definite head by a marked hook and tail and (e2) amorphous head, without hook, banana-shaped, without head and etc. ($\times 1000$). In male mice (15- and 36-day treatment). Values are presented as mean \pm SD of eight mice. * $p < 0.05$; ** $p < 0.01$; *** $p < 0.001$ versus control and # $p < 0.05$; ### $p < 0.01$; #### $p < 0.001$ versus other CNTs groups. CNT: carbon nanotube; SD: standard deviation.

In the present study, carboxyl- and amino-functionalized SWCNTs and MWCNTs were synthesized and characterized by FTIR and zeta potentials. We obtained CNTs in this study similar to our former reported data, and previous TEM imaging analysis showed that obtained CNTs suspension achieved through this method will consist of particles with a size range of almost 1–10 μm .⁵⁹ CNTs lengths

prepared for various applications could be as small as 10–20 nm and extend to several hundreds of microns and even more. Occupational and environmental exposure to CNTs mainly occurs with long CNTs while those prepared for biological applications mostly are in the submicrometer range. However, this classification is not absolutely definite, and therefore, both long and short CNTs must be evaluated for their

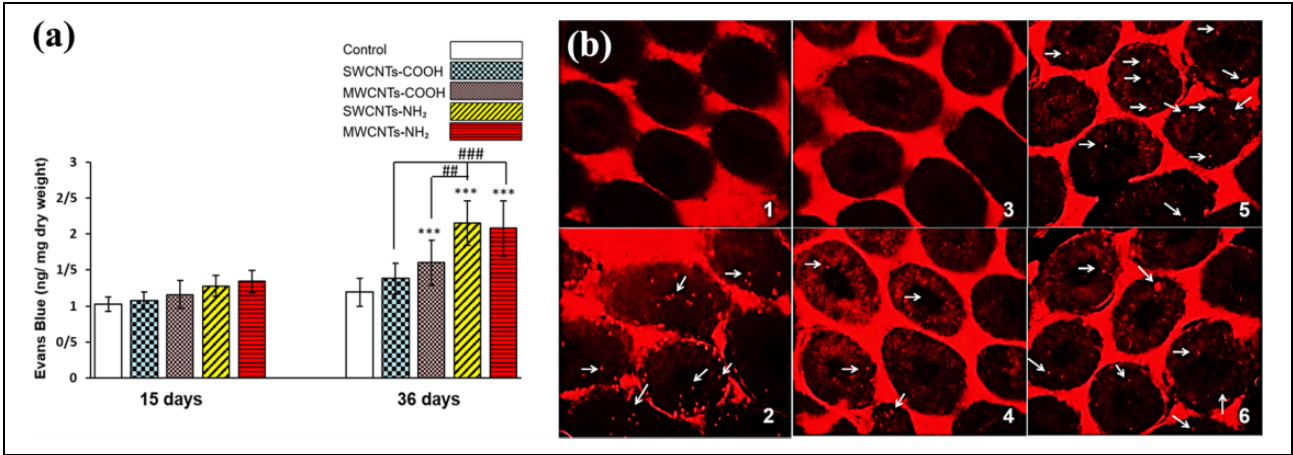


Figure 8. Evans blue extravasation in the testis after CNTs administration. (a) The quantification of Evans blue dye extravasation in the testis at 15- and 36-day treatment of CNTs groups (4 mg/kg, iv) shows an increase in BTB permeability in all groups at 36 days except the SWCNTs-COOH group. (b) Fluorescence images (1 = negative control, 2 = positive control, 3 = SWCNTs-COOH 36 days, 4 = MWCNTs-COOH 36 days, 5 = SWCNTs-NH₂ 36 days, and 6 = MWCNTs-NH₂ 36 days) showed the presence of Evans blue (red) in the seminiferous tubules demonstrating that MWCNTs-COOH, SWCNTs-NH₂, and MWCNTs-NH₂ induces an increase in BTB permeability at 35 days and not in the SWCNTs-COOH and control groups ($\times 100$). The results are expressed as mean \pm SD ($n = 6$). * $p < 0.05$; *** $p < 0.001$, significantly different when compared with control (PBS) and ### $p < 0.01$; #### $p < 0.001$ compared with other CNTs groups. CNT: carbon nanotube; SD: standard deviation; BTB: blood–testis barrier; MWCNT: multiwalled carbon nanotubes; SWCNT: single-walled carbon nanotubes; NH₂: either amine; COOH: carboxylic acid; iv: intravenous; PBS: phosphate-buffered saline.

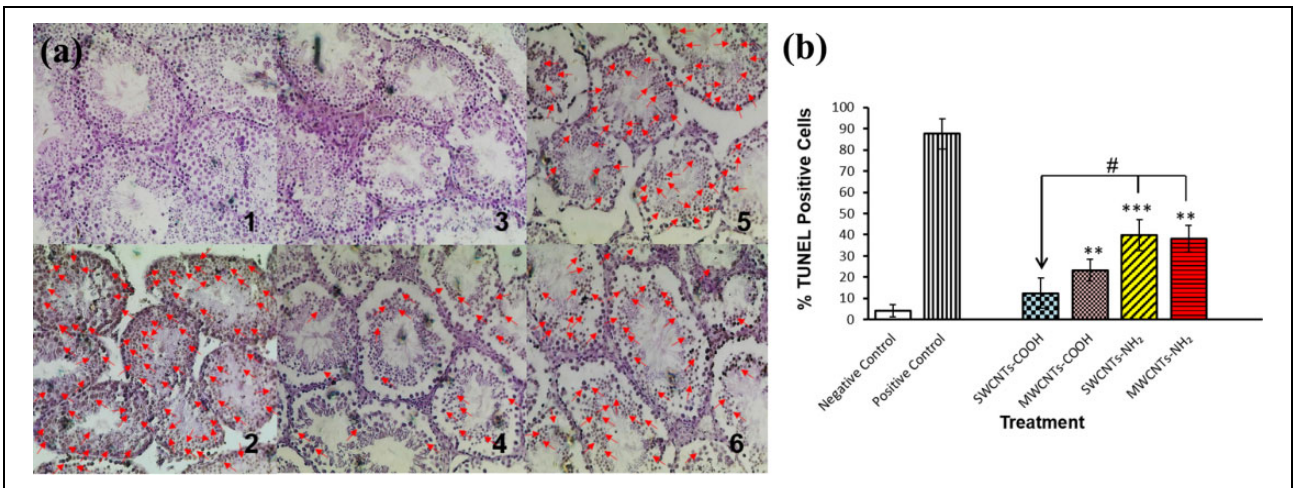


Figure 9. Apoptosis results in mouse testis. (a) TUNEL analysis of testis after iv exposure of CNTs (4 mg/kg) for 36 days (accumulative dose: 24 mg/kg). TUNEL-positive apoptotic cells are stained brown (scale bar 200 \times) and most of them are shown by red arrows. (a1) control, (a2) positive control, (a3) SWCNTs-COOH, (a4) MWCNTs-COOH, (a5) SWCNTs-NH₂, and (a6) MWCNTs-NH₂. (b) Apoptosis rate of the TUNEL assay. Results are expressed as mean \pm SD compared with control groups of the same tissue. ** $p < 0.01$; *** $p < 0.001$ versus negative control and # $p < 0.05$ versus other CNTs groups. TUNEL: terminal deoxynucleotidyl transferase dUTP nick end labeling; CNT: carbon nanotube; SD: standard deviation; MWCNT: multiwalled carbon nanotubes; SWCNT: single-walled carbon nanotubes; NH₂: either amine; COOH: carboxylic acid; iv: intravenous.

effects. For example, most recently, El-Gazzar et al. evaluated the toxic effects of inhaled CNTs almost 7 μm long and examined the effects of the number

of nanotube walls.⁹⁰ Also, in another report, MWCNTs-COOH in the size range of 1–12 μm were administered IP to Wistar rats to evaluate the toxicity

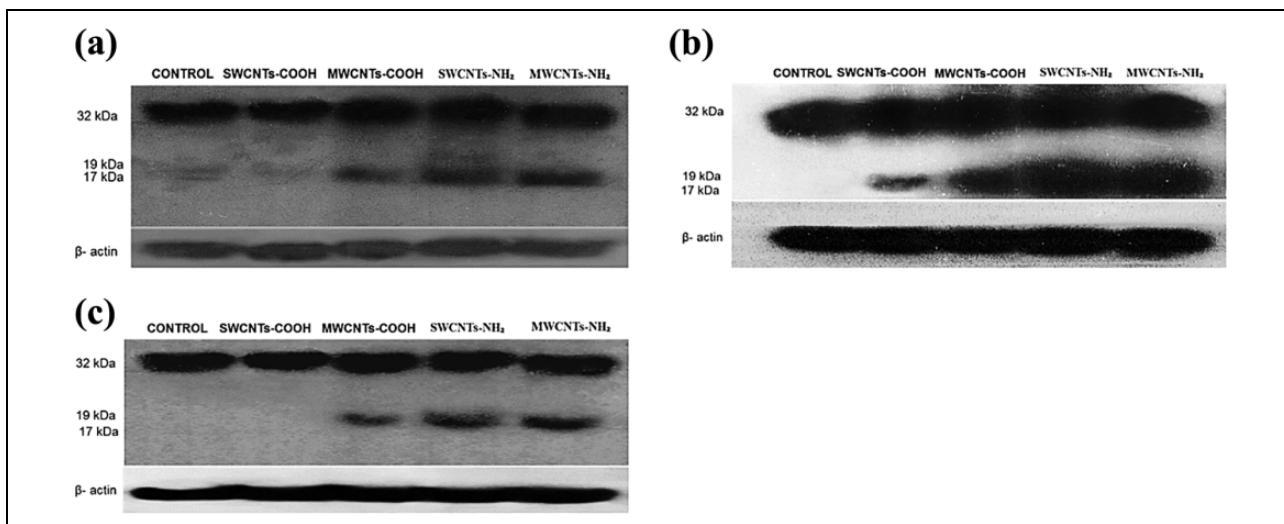


Figure 10. Western blot analysis of caspase-3 protein activation after iv exposure of CNTs (4 mg/kg) for 36 days (accumulative dose: 24 mg/kg) in (a) lung, (b) liver, and (c) testis after treatment with CNTs groups. β -actin was used to verify equal gel loading. CNT: carbon nanotube; iv: intravenous.

in their reproductive systems.⁵⁷ The other pioneer study by Bai et al. also used 0.5–2.0 μm MWCNTs-COOH and MWCNTs-NH₂ through the IV route for further toxicological assessment. Overall, it is evident that more toxicological studies on long and short CNTs are still necessary because of diverse possible routes of human exposure to these nanoparticles and also the diverse types of nanotubes prepared for numerous applications.

In this study, the administration of SWCNTs-COOH and MWCNTs-COOH at different doses (12 and 24 mg/kg) did not affect the normal growth of the treated animals nor did it exhibit any mortality. In contrast, the administration of SWCNTs-NH₂ and MWCNTs-NH₂ at high doses caused a low percentage of mortality, and treated mice showed agitated behavior with an insignificant increase in the relative weights of main target organs (lung, liver, and spleen) in a dose-dependent manner and a significant decrease in total body weight. The significant decrease in total body weight of CNTs-NH₂ can be a simple sign of body toxicity but further investigations are necessary.

Pathological studies indicated dose-dependent moderate and mild changes in CNTs-NH₂- and CNTs-COOH-treated animals in most of the organs mainly after 35 days of treatment. Some organs like kidney and spleen presented only minimal changes. Interestingly, in some samples of the liver, cellular regeneration was also seen. Moreover, simple

morphological data (supporting information) after 5 months after the administration of the final dose showed the exterior color of organs could return to normal state during this time. This might implicate the gradual excretion of nanotubes from the body and provide further evidence for the probable transient effects of nanotubes; however, we did not perform complete pathological studies, and this topic could be examined in future studies for further evaluation.

Oxidative stress is often considered as the main reason for CNTs toxicity.^{34,52} Oxidative stress, the result of dysfunction in antioxidant systems, is defined by overproduction of free oxygen radicals and is one of the major reasons for many diseases and cancers.^{96,97} Earlier reports in cells and mouse models have shown that CNTs could induce oxidative stress in the liver, lung, and spleen after iv injection.⁵¹ Our results were parallel with others as the MDA and carbonyl protein level was significantly higher in CNTs-exposed groups as compared with the control. We propose that CNTs could enhance lipid peroxidation and consequently promote physical changes in the cellular membrane. SOD and GSH were significantly lower in exposed mice compared with the control group in all organs. Although several studies have shown the toxicity of CNTs in vivo and in vitro,^{60,98,99} the mechanisms and the effects of functionalization types remain unknown. Here, we attempted to evaluate the effects of functionalization types on oxidative parameters. Between the two groups of CNTs,

injection of CNTs-NH₂ led to more oxidative stress than the CNTs-COOH group in most of the examined organs. Except in the lung and liver tissue, SWCNTs-COOH was almost nontoxic as oxidative parameters changed nonsignificantly. Therefore, it could be plausible to make more biocompatible CNTs preparations in the future. Much similar to our report, Bai et al. concluded that both carboxylated and aminated MWCNTs could be led to increased oxidative stress and changes in testes. However, the observed data highlighted that there was a mild toxic effect on the male reproductive systems.⁵⁶ Also, Ahmadi et al.⁶⁰ have reported a complete biochemical and proteomic analysis to show that CNTs could alter the cell antioxidant activity although the observed toxicity was not significant. Their data could support our idea that making safe nanotubes is possible, but the possible oxidative stress actions must be considered.

We further examined CNT-induced apoptosis using the caspase-3 assay. Both SWCNTs-NH₂ and MWCNTs-NH₂ groups, after reaching a certain concentration, induced enhanced activation of caspase-3. Also, caspase-3 activation induced by MWCNTs-COOH was significantly milder than that of CNTs-NH₂, and interestingly, in SWCNTs-COOH, no apoptosis or specific pathological effects were observed. The absence of apoptosis and further histopathological findings in the SWCNTs-COOH group was also in parallel with oxidative stress results.

Overall, collecting the data from oxidative stress and caspase-3, we can propose that the observed apoptosis might be the reason of changes in the cellular redox balance. This assumption is showed by both the reduction in the power of antioxidant systems and the increase in reactive oxygen species (ROS) production, which in turn leads to lipid and protein oxidation and, eventually, cell death. Oxidative stress also interferes in cellular signaling pathways which finally exert apoptosis. Also, several *in vitro* toxicity studies of CNTs have shown a correlation between oxidative stress, genotoxicity, and apoptosis in cells.^{46,48,100} In fact, CNTs accumulation in the cell or high CNT concentrations can lead to oxidative stress induction or cell death. Considering lower sedimentation rates in SWCNTs-COOH and better physical stability in comparison to other groups, it could be concluded that the specific parameters of oxidative stress and subsequent cytotoxicity of CNTs might be linked to the physical properties of formulations.³⁹ It must be noted that inflammation, the other parameter of toxicity, can be evaluated in the CNTs studies as it

has been done by many researchers. In this case, the mechanism of CNTs internalization to the cells may play an important role. Indeed when the CNTs with different length sizes (ranging from few several hundred of nanometers to the large several tens of micrometers) are going to have interactions with cell surfaces (as an example typical HeLa cells have 40–70 μm length), various internalization process such as endocytosis or needle-like penetrating process can be suggested.^{101,102} Moreover, it is evident that long and straight fibrous CNTs could elicit an inflammatory response similar to the asbestos fibers especially when they are administered IP or via the pulmonary route. However, the inflammatory response is negligible when the CNTs are small.^{103,104} Indeed morphology and size of CNTs have a determinative role in the immune response, as it was showed by Brown et al.¹⁰⁵ that the short CNTs will be ingested by macrophages and caused a few increase in ROS and tumor necrosis factor-alpha levels in contrast to the long fibrous like CNTs that were associated with a frustrated phagocytosis.

Furthermore, one important aim of the present study was to investigate the influence of carbon nanomaterials on the male reproduction system. Formation of competent spermatozoa is a complex process that is carried out in the seminiferous tubule.¹⁰⁶ Importantly, the BTB constitutes a physical barrier and divides the seminiferous tubules into two different environments, which eventually protects and facilitates the development and differentiation of germ cells into mature spermatids.¹⁰⁷ Germ cells have particular metabolic requirements which make them dependent on Sertoli cells, the structural compartments of the seminiferous tubules.¹⁰⁶ Sperm contain high concentrations of unsaturated fatty acids, so they are very susceptible to oxidative stress while having no capacity for membrane repair and are prone to ROS production.¹⁰⁸ The ROS may affect sperm function via lipoperoxidation-induced changes in membrane integrity and fluidity.¹⁰⁹ Previous to the present study, we have evaluated the *in vitro* toxicity parameters of SWCNTs and MWCNTs on sperm. We concluded that there was no significant difference between SWCNTs and MWCNTs, and both groups showed a decrease in motility but not viability of sperm and also an increase in ROS while not showing negative changes on nitric oxide levels.⁵⁹ Our results indicate an enhancement in testicular ROS generation and lipid peroxidation in CNTs-treated groups in a dose-dependent manner. Relevantly, the increased percentage of immotile

sperm, sperm with abnormal morphology, and also decreased sperm count and viability were recorded following CNTs exposure in the present study. Also, iv injected MWCNTs-COOH and CNTs-NH₂ reduced the integrity of the BTB and induced transient histopathological changes in the testes, but SWCNTs-COOH only reduced motility and viability of sperm. The toxic effects of CNTs are associated with disruption of antioxidant enzyme activities and marked testicular and epididymal dysfunction in the experimental mice. Farombi et al. in a study on male Wistar rats showed that MWCNTs-COOH could increase oxidative stress without affecting sperm characteristics in short-term exposures.⁵⁷ In another study, Bai et al. reported that iv injected MWCNTs-NH₂ and MWCNTs-COOH crossed the BTB and induced histopathological changes in the testis but not in sperm parameters.⁵⁶

Additionally, apoptosis, as identified by TUNEL staining, increased within the seminiferous tubules of mice exposed to CNTs, which was more prominent in the mice treated with CNTs-NH₂. This effect was parallel with the histopathological changes and the intensity of oxidative stress in the testes. The caspase-3 survey also showed similar results. These correlations suggest that CNTs-induced cellular apoptosis in testes might originate from an imbalance in the antioxidant pathways and subsequent lipid and protein oxidation. Again, in this study, a trend similar to previous tests was observed for SWCNT-COOH, as it did not increase the TUNEL positive cells significantly and can be regarded as the safest group among all CNTs-treated groups.

Conclusions

The present study examines the acute and chronic toxicological effects of CNTs on important organs, especially in the male reproductive system, in terms of functionalization type and nanotube layers. CNTs were able to increase the oxidative stress parameters as well as deplete GSH and SOD. The effects were more severe in the chronic phase as compared with the acute phase. The observed toxicity was correlated with apoptosis, as revealed by caspase 3 activation and TUNEL test. We showed that the functionalization of nanotubes with carboxylic derivatives could lead to more biocompatible delivery cargos in comparison with the CNTs-NH₂. Another observation in this study was that although not significant in all tests, single-walled nanotubes did show lower overall toxicity in comparison to multiwalled nanotubes. In this

study, SWCNTs-COOH showed the least toxicity, and in many parameters, it did not cause any significant change in toxicity parameters or the male reproductive system. The higher biocompatibility of SWCNTs-COOH might be related, in part, to its better physical stability, but we did not perform complete stability tests. Also, the utilized nanotubes in this study had a size of almost 10 μm, and we did not evaluate the effects of shorter CNTs. Interestingly, our preliminary study showed that the color of the animal's organs could be turned back to a somewhat normal state 5 months after the administration of the final dose, and this might be a sign of CNTs excretion. We believe that further studies shedding light on the routes and mechanisms at work in CNT excretion may pave the way to producing safer and more effective nanotubes in the future.

Acknowledgments

The authors would like to acknowledge the Pharmaceutics Research Center and the Kerman University of Medical Sciences for their financial support (reference number: 97000304) of this study. Also, the Research Institute of Petroleum Industry (RIPI) is gratefully acknowledged for their kind donation of nanotubes.

Declaration of conflicting interests

The author(s) declared no potential conflicts of interest with respect to the research, authorship, and/or publication of this article.

Funding

The author(s) disclosed receipt of the following financial support for the research, authorship, and/or publication of this article: The authors gratefully acknowledge the financial support from the Kerman University of Medical Sciences (Grant Number 97000304).

Supplemental material

Supplemental material for this article is available online.

References

1. Caster JM, Patel AN, Zhang T, et al. Investigational nanomedicines in 2016: a review of nanotherapeutics currently undergoing clinical trials. *Wiley Interdiscip Rev Nanomed Nanobiotechnol* 2017; 9(1): e1416.
2. Mohammadinejad R, Dadashzadeh A, Moghassemi S, et al. Shedding light on gene therapy: carbon dots for the minimally invasive image-guided delivery of plasmids and noncoding RNAs. *J Adv Res* 2019; 18: 81–93.

3. Mohammadinejad R, Moosavi MA, Tavakol S, et al. Necrotic, apoptotic and autophagic cell fates triggered by nanoparticles. *Autophagy*. 2019; 15: 4–33.
4. Eivazzadeh-Keihan R, Maleki A, de la Guardia M, et al. Carbon based nanomaterials for tissue engineering of bone: building new bone on small black scaffolds: a review. *J Adv Res* 2019; 18: 185–201.
5. Chenab KK, Eivazzadeh-Keihan R, Maleki A, et al. Biomedical applications of nanoflares: targeted intracellular fluorescence probes. *Nanomed Nanotechnol Biol Med*. 2019; 17: 342–358.
6. Afsharzadeh M, Hashemi M, Mokhtarzadeh A, et al. Recent advances in co-delivery systems based on polymeric nanoparticle for cancer treatment. *Artif Cells Nanomed Biotechnol* 2018; 46: 1095–1110.
7. Eivazzadeh-Keihan R, Pashazadeh-Panahi P, Baradaran B, et al. Recent advances on nanomaterial based electrochemical and optical aptasensors for detection of cancer biomarkers. *TrAC Trends Analyt Chem* 2018; 100: 103–115.
8. Ajdary M, Moosavi M, Rahmati M, et al. Health concerns of various nanoparticles: a review of their in vitro and in vivo toxicity. *Nanomaterials*. 2018; 8: 634.
9. Duncan R and Gaspar R. Nanomedicine (s) under the microscope. *Molr Pharm* 2011; 8: 2101–2141.
10. Behnam B, Rezazadehkermani M, Ahmadzadeh S, et al. Microniosomes for concurrent doxorubicin and iron oxide nanoparticles loading; preparation, characterization and cytotoxicity studies. *Artif Cells Nanomed Biotechnol* 2018; 46: 118–125.
11. Nadimi AE, Ebrahimipour SY, Afshar EG, et al. Nano-scale drug delivery systems for antiarrhythmic agents. *Eur J Med Chem* 2018; 157: 1153–1163.
12. Ahmadi Z, Mohammadinejad R and Ashrafzadeh M. Drug delivery systems for resveratrol, a non-flavonoid polyphenol: emerging evidence in last decades. *J Drug Deliv Sci Technol* 2019; 51: 591–604.
13. He H, Xiao D, Pham-Huy LA, et al. Carbon nanotubes used as nanocarriers in drug and biomolecule delivery. In: Keservani RK, Sharma AK and Kesharwani RK (eds) *Drug Delivery Approaches and Nanosystems*. 1st ed, Vol. 1. New York: Apple Academic press, 2017, pp. 163–212.
14. Mohajeri M, Behnam B and Sahebkar A. Biomedical applications of carbon nanomaterials: drug and gene delivery potentials. *J Cell physiol* 2018; 234: 298–319.
15. Rezaee M, Behnam B, Banach M, et al. The Yin and Yang of carbon nanomaterials in atherosclerosis. *Bio-technol Adv* 2018; 36: 2232–2247.
16. Mohajeri M, Behnam B, Barreto GE, et al. Carbon nanomaterials and amyloid-beta interactions: potentials for the detection and treatment of Alzheimer's disease? *Pharmacol Res* 2019; 143: 186–203.
17. Rezaei M, Mahmoodi P, Langari H, et al. Conjugates of curcumin with graphene and carbon nanotubes: a review on biomedical applications. *Current Medicinal Chemistry*. Epub ahead of print 2019. DOI: 10.2174/0929867326666191113145745.
18. Teradal NL and Jelinek R. Carbon nanomaterials in biological studies and biomedicine. *Adv Healthc Mater* 2017; 6: 1700574.
19. Saito N, Haniu H, Usui Y, et al. Safe clinical use of carbon nanotubes as innovative biomaterials. *Chem Rev* 2014; 114: 6040–6079.
20. Oloumi H, Mousavi EA and Nejad RM. Multi-wall carbon nanotubes effects on plant seedlings growth and cadmium/lead uptake in vitro. *Russ J Plant Physiol* 2018; 65: 260–268.
21. Takeuchi T, Iizumi Y, Yudasaka M, et al. Characterization and biodistribution analysis of oxygen-doped single-walled carbon nanotubes used as in vivo fluorescence imaging probes. *Bioconjugate Chem* 2019; 30: 1323–1330.
22. Zhang T, Tang M, Zhang S, et al. Systemic and immunotoxicity of pristine and PEGylated multi-walled carbon nanotubes in an intravenous 28 days repeated dose toxicity study. *Int J Nanomed* 2017; 12: 1539.
23. Liu X, Tao H, Yang K, et al. Optimization of surface chemistry on single-walled carbon nanotubes for in vivo photothermal ablation of tumors. *Biomaterials*. 2011; 32: 144–151.
24. Ali-Boucetta H and Kostarelos K. Pharmacology of carbon nanotubes: toxicokinetics, excretion and tissue accumulation. *Adv Drug Deliv Rev* 2013; 65: 2111–2119.
25. Segawa Y, Ito H and Itami K. Structurally uniform and atomically precise carbon nanostructures. *Nat Rev Mater* 2016; 1: 15002.
26. Hosnedlova B, Kepinska M, Fernandez C, et al. Carbon nanomaterials for targeted cancer therapy drugs: a critical review. *Chem Rec* 2019; 19: 502–522.
27. Li Z, Fan J, Tong C, et al. A smart drug-delivery nano-system based on carboxylated graphene quantum dots for tumor-targeted chemotherapy. *Nanomedicine* 2019; 14(15): 2011–2025.
28. Cao Y, Huang HY, Chen LQ, et al. Enhanced lysosomal escape of pH-responsive polyethylenimine–betaine functionalized carbon nanotube for the codelivery of survivin small interfering RNA and doxorubicin. *ACS Appl Mater Interfaces* 2019; 11: 9763–9776.

29. Sheikhpour M, Golbabaie A and Kasaeian A. Carbon nanotubes: a review of novel strategies for cancer diagnosis and treatment. *Mater Sci Eng: C*. 2017; 76: 1289–1304.
30. Yousefi M, Dadashpour M, Hejazi M, et al. Anti-bacterial activity of graphene oxide as a new weapon nanomaterial to combat multidrug-resistance bacteria. *Mater Sci Eng C* 2017; 74: 568–581.
31. Hirschfeld J, Akinoglu EM, Wirtz DC, et al. Long-term release of antibiotics by carbon nanotube-coated titanium alloy surfaces diminish biofilm formation by *Staphylococcus epidermidis*. *Nanomed Nanotechnol Biol Med*. 2017; 13: 1587–1593.
32. Hashem Nia A, Behnam B, Taghavi S, et al. Evaluation of chemical modification effects on DNA plasmid transfection efficiency of single-walled carbon nanotube-succinate-polyethylenimine conjugates as non-viral gene carriers. *Med Chem Comm*. 2017; 8: 364–375.
33. Behnam B, Shier WT, Nia AH, et al. Non-covalent functionalization of single-walled carbon nanotubes with modified polyethyleneimines for efficient gene delivery. *Int J Pharm*. 2013; 454: 204–215.
34. Balasubramanian K and Burghard M. Chemically functionalized carbon nanotubes. *Small*. 2005; 1: 180–192.
35. Osorio A, Silveira I, Bueno V, et al. H₂SO₄/HNO₃/HCl—functionalization and its effect on dispersion of carbon nanotubes in aqueous media. *Appl Surf Sci* 2008; 255: 2485–2489.
36. Marshall MW, Popa-Nita S and Shapter JG. Measurement of functionalised carbon nanotube carboxylic acid groups using a simple chemical process. *Carbon*. 2006; 44: 1137–1341.
37. Ramanathan T, Fisher F, Ruoff R, et al. Amino-functionalized carbon nanotubes for binding to polymers and biological systems. *Chem Mater* 2005; 17: 1290–1295.
38. Stern ST and McNeil SE. Nanotechnology safety concerns revisited. *Toxicolog Sci* 2007; 101: 4–21.
39. Nymark P, Jensen KA, Suhonen S, et al. Free radical scavenging and formation by multi-walled carbon nanotubes in cell free conditions and in human bronchial epithelial cells. *Part Fibre Toxicol* 2014; 11: 4.
40. Firme CP and Bandaru PR. Toxicity issues in the application of carbon nanotubes to biological systems. *Nanomed Nanotechnol Biol Med* 2010; 6: 245–256.
41. Chatterjee N, Yang J, Kim H-M, et al. Potential toxicity of differential functionalized multiwalled carbon nanotubes (MWCNT) in human cell line (BEAS2B) and *Caenorhabditis elegans*. *J Toxicol Environ Health Part A*. 2014; 77: 1399–1408.
42. Sturm R. Carbon nanotubes in the human respiratory tract—clearance modeling. *Annals of Work Exposures and Health*. 2017; 61: 226–236.
43. Silva RM, Doudrick K, Franzi LM, et al. Instillation versus inhalation of multiwalled carbon nanotubes: exposure-related health effects, clearance, and the role of particle characteristics. *ACS Nano*. 2014; 8: 8911–8931.
44. Dong J and Ma Q. Suppression of basal and carbon nanotube-induced oxidative stress, inflammation and fibrosis in mouse lungs by Nrf2. *Nanotoxicology*. 2016; 10: 699–709.
45. Hu X, Ouyang S, Mu L, et al. Effects of graphene oxide and oxidized carbon nanotubes on the cellular division, microstructure, uptake, oxidative stress, and metabolic profiles. *Environ Sci Technol* 2015; 49: 10825–10833.
46. Dinicola S, Masiello MG, Proietti S, et al. Multiwalled carbon nanotube buckypaper induces cell cycle arrest and apoptosis in human leukemia cell lines through modulation of AKT and MAPK signaling pathways. *Toxicol Vitro*. 2015; 29: 1298–1308.
47. Zeni O, Sannino A, Romeo S, et al. Growth inhibition, cell-cycle alteration and apoptosis in stimulated human peripheral blood lymphocytes by multiwalled carbon nanotube buckypaper. *Nanomedicine*. 2015; 10: 351–360.
48. Lee JW, Choi YC, Kim R, et al. Multiwall carbon nanotube-induced apoptosis and antioxidant gene expression in the gills, liver, and intestine of *Oryzias latipes*. *BioMed Res Int* 2015; 2015: 10.
49. Rahman L, Jacobsen NR, Aziz SA, et al. Multi-walled carbon nanotube-induced genotoxic, inflammatory and pro-fibrotic responses in mice: investigating the mechanisms of pulmonary carcinogenesis. *Mutat Res/Genetic Toxicol Environ Mutagen* 2017; 823: 28–44.
50. Khaliullin TO, Kisin ER, Murray AR, et al. Mediation of the single-walled carbon nanotubes induced pulmonary fibrogenic response by osteopontin and TGF- β 1. *Exper Lung Res* 2017; 43: 311–326.
51. Qin Y, Li S, Zhao G, et al. Long-term intravenous administration of carboxylated single-walled carbon nanotubes induces persistent accumulation in the lungs and pulmonary fibrosis via the nuclear factor-kappa B pathway. *Int J Nanomed* 2017; 12: 263.
52. Lan Z and Yang W-X. Nanoparticles and spermatogenesis: how do nanoparticles affect spermatogenesis and penetrate the blood–testis barrier. *Nanomedicine*. 2012; 7: 579–596.

53. Yoshida S, Hiyoshi K, Oshio S, et al. Effects of fetal exposure to carbon nanoparticles on reproductive function in male offspring. *Fertil Steril* 2010; 93: 1695–1699.
54. Vasyukova I, Gusev A and Tkachev A. Reproductive toxicity of carbon nanomaterials: a review. *IOP Conference Series: Materials Science and Engineering* 2015; 98: 012001.
55. Ema M, Hougaard KS, Kishimoto A, et al. Reproductive and developmental toxicity of carbon-based nanomaterials: a literature review. *Nanotoxicology*. 2016; 10: 391–412.
56. Bai Y, Zhang Y, Zhang J, et al. Repeated administrations of carbon nanotubes in male mice cause reversible testis damage without affecting fertility. *Nat Nanotechnol* 2010; 5: 683.
57. Farombi EO, Adedara IA, Forcados GE, et al. Responses of testis, epididymis, and sperm of pubertal rats exposed to functionalized multiwalled carbon nanotubes. *Environ Toxicol* 2016; 31: 543–551.
58. Bonde JP. Male reproductive organs are at risk from environmental hazards. *Asian J Androl* 2010; 12: 152.
59. Aminzadeh Z, Jamal M, Chupani L, et al. In vitro reprotoxicity of carboxyl-functionalised single- and multi-walled carbon nanotubes on human spermatozoa. *Andrologia* 2017; 49: e12741.
60. Ahmadi H, Ramezani M, Yazdian-Robati R, et al. Acute toxicity of functionalized single wall carbon nanotubes: a biochemical, histopathologic and proteomics approach. *Chem Biol Interact* 2017; 275: 196–209.
61. Hong SY, Tobias G, Al-Jamal KT, et al. Filled and glycosylated carbon nanotubes for in vivo radioemitter localization and imaging. *Nat Mater* 2010; 9: 485.
62. Liu Z, Davis C, Cai W, et al. Circulation and long-term fate of functionalized, biocompatible single-walled carbon nanotubes in mice probed by Raman spectroscopy. *Proceed Natl Acad Sci* 2008; 105: 1410–1415.
63. Yang S-T, Wang X, Jia G, et al. Long-term accumulation and low toxicity of single-walled carbon nanotubes in intravenously exposed mice. *Toxicol Lett* 2008; 181: 182–189.
64. Pourgholamhossein F, Rasooli R, Pournamdari M, et al. Pirfenidone protects against paraquat-induced lung injury and fibrosis in mice by modulation of inflammation, oxidative stress, and gene expression. *Food Chem Toxicol* 2018; 112: 39–46.
65. Bradford MM. A rapid and sensitive method for the quantitation of microgram quantities of protein utilizing the principle of protein-dye binding. *Analyt Biochem* 1976; 72: 248–254.
66. Jiang W-D, Feng L, Liu Y, et al. Lipid peroxidation, protein oxidant and antioxidant status of muscle, intestine and hepatopancreas for juvenile Jian carp (*Cyprinus Carpio* var. Jian) fed graded levels of myo-inositol. *Food Chem* 2010; 120: 692–697.
67. Ohkawa H, Ohishi N and Yagi K. Assay for lipid peroxides in animal tissues by thiobarbituric acid reaction. *Analyt Biochem* 1979; 95: 351–358.
68. Levine RL, Garland D, Oliver CN, et al. *Determination of carbonyl content in oxidatively modified proteins. Methods in enzymology*. Amsterdam: Elsevier, 1990, p. 464–478.
69. Shojaeepour S, Fazeli M, Oghabian Z, et al. Oxidative stress in opium users after using lead-adulterated opium: the role of genetic polymorphism. *Food Chem Toxicol* 2018; 120: 571–577.
70. Marklund S and Marklund G. Involvement of the superoxide anion radical in the autoxidation of pyrogallol and a convenient assay for superoxide dismutase. *FEBS J* 1974; 47: 469–474.
71. Pourgholamhossein F, Sharififar F, Rasooli R, et al. Thymoquinone effectively alleviates lung fibrosis induced by paraquat herbicide through down-regulation of pro-fibrotic genes and inhibition of oxidative stress. *Environ Toxicol Pharmacol* 2016; 45: 340–345.
72. Hu ML. *Measurement of protein thiol groups and glutathione in plasma. Methods in enzymology*. Amsterdam: Elsevier, 1994, p. 380–385.
73. Mandegary A, Sezavar M, Saeedi A, et al. Oxidative stress induced in the workers of natural gas refineries, no role for GSTM1 and GSTT1 polymorphisms. *Human Exper Toxicol* 2012; 31: 1271–1279.
74. Khorsandi L, Hashemitabar M, Orazizadeh M, et al. Dexamethasone effects on fas ligand expression in mouse testicular germ cells. *Pak J Biol Sci PJBs*. 2008; 11: 2231–2236.
75. Yan J-G, Agresti M, Bruce T, et al. Effects of cellular phone emissions on sperm motility in rats. *Fertil Steril* 2007; 88: 957–964.
76. Cooper TG, Noonan E, Von Eckardstein S, et al. World Health Organization reference values for human semen characteristics. *Hum Reprod Update* 2010; 16: 231–245.
77. Björndahl L, Söderlund I and Kvist U. Evaluation of the one-step eosin-nigrosin staining technique for human sperm vitality assessment. *Human Reprod* 2003; 18: 813–816.

78. Barakat R, Lin P-CP, Rattan S, et al. Prenatal exposure to DEHP induces premature reproductive senescence in male mice. *Toxicol Sci* 2017; 156: 96–108.
79. Emanuelli C, Grady EF, Madeddu P, et al. Acute ACE inhibition causes plasma extravasation in mice that is mediated by bradykinin and substance P. *Hypertension*. 1998; 31: 1299–1304.
80. Mohammadi-Sardoo M, Mandegary A, Nabiuni M, et al. Mancozeb induces testicular dysfunction through oxidative stress and apoptosis: protective role of N-acetylcysteine antioxidant. *Toxicol Ind Health* 2018; 34: 798–811.
81. Eatemadi A, Daraee H, Karimkhanloo H, et al. Carbon nanotubes: properties, synthesis, purification, and medical applications. *Nanoscale Res Lett* 2014; 9: 393.
82. Marchesan S, Kostarelos K, Bianco A, et al. The winding road for carbon nanotubes in nanomedicine. *Mater Today* 2015; 18: 12–19.
83. Puett C, Insoe C, Hartman A, et al. An update on carbon nanotube-enabled X-ray sources for biomedical imaging. *Wiley Interdiscip Rev Nanomed Nanobiotechnol* 2018; 10: e1475. Epub 2017.
84. Sobhani Z, Behnam MA, Emami F, et al. Photothermal therapy of melanoma tumor using multiwalled carbon nanotubes. *Int J Nanomed* 2017; 12: 4509.
85. Arora S, Kumar R, Kaur H, et al. Translocation and toxicity of docetaxel multi-walled carbon nanotube conjugates in mammalian breast cancer cells. *J Biomed Nanotechnol* 2014; 10: 3601–3609.
86. Amenta V and Aschberger K. Carbon nanotubes: potential medical applications and safety concerns. *Wiley Interdiscip Rev Nanomed Nanobiotechnol* 2015; 7: 371–386.
87. Montes-Fonseca SL, Orrantia-Borunda E, Aguilar-Elgueabal A, et al. Cytotoxicity of functionalized carbon nanotubes in J774A macrophages. *Nanomed Nanotechnol Biol Med* 2012; 8: 853–859.
88. Mehra NK and Jain NK. Multifunctional hybrid-carbon nanotubes: new horizon in drug delivery and targeting. *J Drug Target* 2016; 24: 294–308.
89. Ursini CL, Maiello R, Ciervo A, et al. Evaluation of uptake, cytotoxicity and inflammatory effects in respiratory cells exposed to pristine and-OH and-COOH functionalized multi-wall carbon nanotubes. *J Appl Toxicol* 2016; 36: 394–403.
90. El-Gazzar AM, Abdelgied M, Alexander DB, et al. Comparative pulmonary toxicity of a DWCNT and MWCNT-7 in rats. *Arch Toxicol* 2019; 93(1): 49–59. Epub 2018.
91. Dyke CA and Tour JM. Covalent functionalization of single-walled carbon nanotubes for materials applications. *J Phys Chem A*. 2004; 108: 11151–11159.
92. Kim SW, Kim T, Kim YS, et al. Surface modifications for the effective dispersion of carbon nanotubes in solvents and polymers. *Carbon* 2012; 50: 3–33.
93. Kostarelos K, Bianco A and Prato M. Promises, facts and challenges for carbon nanotubes in imaging and therapeutics. *Nat Nanotechnol* 2009; 4: 627–633.
94. Liu Z, Liu Y and Peng D. Carboxylation of multiwalled carbon nanotube attenuated the cytotoxicity by limiting the oxidative stress initiated cell membrane integrity damage, cell cycle arrestment, and death receptor mediated apoptotic pathway. *J Biomed Mater Res Part A*. 2015; 103: 2770–2777.
95. Saxena RK, Williams W, Mcgee JK, et al. Enhanced in vitro and in vivo toxicity of poly-dispersed acid-functionalized single-wall carbon nanotubes. *Nanotoxicology*. 2007; 1: 291–300.
96. Lawson M, Jomova K, Poprac P, et al. Free radicals and antioxidants in human disease. In: Al-Gubory K and Laher I (eds) *Nutritional Antioxidant Therapies: Treatments and Perspectives*. 1st ed. Switzerland (Cham): Springer, 2017, pp. 283–307.
97. Bhat AH, Dar KB, Anees S, et al. Oxidative stress, mitochondrial dysfunction and neurodegenerative diseases; a mechanistic insight. *Biomed Pharmacother* 2015; 74: 101–110.
98. Awasthi KK, John P, Awasthi A, et al. Multi walled carbon nano tubes induced hepatotoxicity in Swiss albino mice. *Micron* 2013; 44: 359–364.
99. Cheng C, Müller KH, Koziol KK, et al. Toxicity and imaging of multi-walled carbon nanotubes in human macrophage cells. *Biomaterials* 2009; 30: 4152–4160.
100. Bottini M, Bruckner S, Nika K, et al. Multi-walled carbon nanotubes induce T lymphocyte apoptosis. *Toxicol Lett* 2006; 160: 121–126.
101. Lacerda L, Raffa S, Prato M, et al. Cell-penetrating CNTs for delivery of therapeutics. *Nano Today*. 2007; 2: 38–43.
102. Yehia HN, Draper RK, Mikoryak C, et al. Single-walled carbon nanotube interactions with HeLa cells. *J Nanobiotechnol* 2007; 5: 8.
103. Murphy FA, Poland CA, Duffin R, et al. Length-dependent retention of carbon nanotubes in the pleural space of mice initiates sustained inflammation and progressive fibrosis on the parietal pleura. *Am J Pathol* 2011; 178: 2587–2600.

104. Poland CA, Duffin R, Kinloch I, et al. Carbon nanotubes introduced into the abdominal cavity of mice show asbestos-like pathogenicity in a pilot study. *Nat Nanotechnol* 2008; 3: 423.
105. Brown D, Kinloch I, Bangert U, et al. An in vitro study of the potential of carbon nanotubes and nanofibres to induce inflammatory mediators and frustrated phagocytosis. *Carbon* 2007; 45: 1743–1756.
106. Mruk DD and Cheng CY. Sertoli-Sertoli and Sertoli-germ cell interactions and their significance in germ cell movement in the seminiferous epithelium during spermatogenesis. *Endocr Rev* 2004; 25: 747–806.
107. Dym M and Fawcett DW. The blood-testis barrier in the rat and the physiological compartmentation of the seminiferous epithelium. *Biol Reprod* 1970; 3: 308–326.
108. Aitken RJ, Smith TB, Jobling MS, et al. Oxidative stress and male reproductive health. *Asian J Androl* 2014; 16: 31.
109. Khan S, Jan M, Kumar D, et al. Firpronil induced spermotoxicity is associated with oxidative stress, DNA damage and apoptosis in male rats. *Pestic Biochem Physiol* 2015; 124: 8–14.